



HAL
open science

Regional vegetation and climate changes during the last 13 kyr from a marine pollen record in Seno Reloncaví, southern Chile

Vincent Montade, Nathalie Combourieu Nebout, Emmanuel Chapron, Sandor Mulsow, Ana M. Abarzua, Maxime Debret, Anthony Foucher, Marc Desmet, Thierry Winiarski, Catherine Kissel

► To cite this version:

Vincent Montade, Nathalie Combourieu Nebout, Emmanuel Chapron, Sandor Mulsow, Ana M. Abarzua, et al.. Regional vegetation and climate changes during the last 13 kyr from a marine pollen record in Seno Reloncaví, southern Chile. *Review of Palaeobotany and Palynology*, 2012, 181, pp.11-21. 10.1016/j.revpalbo.2012.04.005 . insu-00691601

HAL Id: insu-00691601

<https://insu.hal.science/insu-00691601>

Submitted on 21 May 2013

HAL is a multi-disciplinary open access archive for the deposit and dissemination of scientific research documents, whether they are published or not. The documents may come from teaching and research institutions in France or abroad, or from public or private research centers.

L'archive ouverte pluridisciplinaire **HAL**, est destinée au dépôt et à la diffusion de documents scientifiques de niveau recherche, publiés ou non, émanant des établissements d'enseignement et de recherche français ou étrangers, des laboratoires publics ou privés.

**Regional vegetation and climate changes during the last 13 kyr from a marine pollen record
in Seno Reloncaví, southern Chile**

*Vincent Montade (1, 2)

vincent.montade@laposte.net

Laboratoire des Sciences du Climat et de l'Environnement (LSCE), UMR 8212
CNRS/UVSQ/CEA, Orme des Merisiers, 91191 Gif-sur-Yvette, France

Institut des Sciences de l'Evolution de Montpellier (ISE-M), UMR 226 IRD/CNRS/UMII, Place
Eugène Bataillon, 34095 Montpellier, France

Nathalie Combourieu Nebout (1)

nathalie.nebout@lsce.ipsl.fr

Laboratoire des Sciences du Climat et de l'Environnement (LSCE), UMR 8212
CNRS/UVSQ/CEA, Orme des Merisiers, 91191 Gif-sur-Yvette, France

Emmanuel Chapron (3)

emmanuel.chapron@univ-orleans.fr

Institut des Sciences de la Terre d'Orléans (ISTO), UMR 7327 CNRS/Université d'Orléans, 1A rue
de la Férollerie, 45071 Orléans, France

Sandor Mulsow (4)

sandormulsow@gmail.com

Instituto de Geociencias, Universidad Austral de Chile, Valdivia, Chile

Ana M. Abarzúa (5)

anaabarzua@uach.cl

Instituto de Ciencias Ambientales y Evolutivas, Universidad Austral de Chile, Valdivia, Chile

Maxime Debret (6)

maximedebret@yahoo.fr

Laboratoire de Météorologie Dynamique (LMD) & CERES-ERTI (IPSL), UMR 8539, Ecole Normale Supérieure, 24, Rue Lhomond, 75231, Paris, France

Anthony Foucher (3, 7)

anthony.foucher@etu.univ-tours.fr

Institut des Sciences de la Terre d'Orléans (ISTO), UMR 7327 CNRS/Université d'Orléans, 1A rue de la Férollerie, 45071 Orléans cedex 2, France

Laboratoire GéHCO, Faculté des Sciences et Techniques, Université François Rabelais, Parc de Grandmont, 37200 Tours, France

Marc Desmet (7)

marc.desmet@univ-tours.fr

Laboratoire GéHCO, Faculté des Sciences et Techniques, Université François Rabelais, Parc de Grandmont, 37200 Tours, France

Thierry Winiarski (8)

Thierry.WINIARSKI@entpe.fr

Ecole Nationale des Travaux Publics de l'Etat (ENTPE), UMR 5023 LEHN/IPE, Université de Lyon, Rue M. Audin, 68518 Vaulx en Velin, France

Catherine Kissel (9)

Catherine.Kissel@lsce.ipsl.fr

Laboratoire des Sciences du Climat et de l'Environnement (LSCE), UMR 8212
CNRS/UVSQ/CEA, Bât. 12, Avenue de la Terrasse, 91198 Gif-sur-Yvette, France

(1) Laboratoire des Sciences du Climat et de l'Environnement (LSCE), UMR 8212
CNRS/UVSQ/CEA, Orme des Merisiers, 91191 Gif-sur-Yvette, France

(2) Institut des Sciences de l'Evolution de Montpellier (ISE-M), UMR 226 IRD/CNRS/UMII, Place
Eugène Bataillon, 34095 Montpellier, France

(3) Institut des Sciences de la Terre d'Orléans (ISTO), UMR 7327 CNRS/Université d'Orléans, 1A
rue de la Férollerie, 45071 Orléans, France

(4) Instituto de Geociencias, Universidad Austral de Chile, Valdivia, Chile

(5) Instituto de Ciencias Ambientales y Evolutivas, Universidad Austral de Chile, Valdivia, Chile

(6) Laboratoire de Météorologie Dynamique (LMD) & CERES-ERTI (IPSL), UMR 8539, Ecole
Normale Supérieure, 24, Rue Lhomond, 75231, Paris, France

(7) Laboratoire GÉHCO, Faculté des Sciences et Techniques, Université François Rabelais, Parc de
Grandmont, 37200 Tours, France

(8) Ecole Nationale des Travaux Publics de l'Etats (ENTPE), UMR 5023 LEHN/IPE, Université de
Lyon, Rue M. Audin, 68518 Vaulx en Velin, France

(9) Laboratoire des Sciences du Climat et de l'Environnement (LSCE), UMR 8212
CNRS/UVSQ/CEA, Bât. 12, Avenue de la Terrasse, 91198 Gif-sur-Yvette, France

*** Corresponding author**

Vincent Montade

Abstract

A marine pollen record from Seno Reloncaví (southern Chile, 41°S) illustrates temperate rainforest changes during the last 13 cal kyr BP. Our study shows the end of the last Termination at ~11.5-12 cal kyr BP coincident with the expansion of *Weinmannia*, illustrating disturbance and warming conditions, at the expense of cold-resistant conifers (*Fitzroya-Pilgerodendron* and *Podocarpus*). Warming conditions are strengthened at 10.7 cal kyr BP by the increase of heliophytic taxa (*Eucryphia-Caldcluvia*) characteristic of the Valdivian rainforest. These heliophytic taxa reach their maximum expansion between 9.6 and 7.4 cal kyr BP and point to warm and dry conditions during the Holocene Climatic Optimum. After 7.4 cal kyr BP, vegetation changes indicate variable climate conditions superimposed on a cooling trend associated with an increase in precipitation after ~6-5 cal kyr BP, shown by the expansion of the cold-resistant conifers. During the late Holocene, after 2.8 cal kyr BP, the continuous expansion of cold-resistant conifers marks an increase of cool and wet conditions. The comparison between marine and terrestrial pollen records highlights the similar trends and timing of vegetation changes that allows to complete the regional pattern of vegetation changes around Seno Reloncaví. In comparison with the terrestrial pollen records, this marine pollen record provides a more regional signal of vegetation/climate changes and clearly demonstrates the sensitivity of marine pollen records to past vegetation and climate change.

Keyword

Southern hemisphere; Patagonia; palaeoenvironment; Holocene; rainforest; pollen; marine core

1. Introduction

In the context of climate change (IPCC, 2007), palaeoclimate records at different temporal and spatial scales are crucial for understanding climate mechanisms. Southern South America, crossed by the Andes from north to south, is a critical topographic constraint on the atmospheric and oceanographic systems and represents the only continental land mass intercepting the entire southern westerly wind belt in the southern hemisphere. Therefore, southern Chile is a key area for the study of palaeoenvironmental changes in the southern hemisphere and the understanding of ocean-atmosphere mechanisms and their interactions with the mid- to high-latitudes of the southern hemisphere. Over the last few decades, northwestern Patagonia, one of the most studied regions of southern South America, produced numerous terrestrial pollen records from peat bogs or lake sediments used to reconstruct past vegetation and climate changes (e.g. Heusser, 1966; Villagrán, 1980, 1988a, 1988b; Heusser et al., 1981, 1996; Moreno, 1997, 2004; Moreno et al., 2001, 1999; Markgraf et al., 2002; Moreno and León, 2003; Abarzúa et al., 2004; Abarzúa and Moreno, 2008; Vargas-Ramirez et al., 2008). Pollen records during the last Termination (e.g. Heusser, 1966; Villagrán, 1988b; Heusser et al., 1996; Moreno, 2004; Abarzúa et al., 2004; Vargas-Ramirez et al., 2008), show temperate rainforest expansion following the glacial retreat recorded at 17.8 cal kyr BP in the region of the Chilean Lake District and Isla Grande de Chiloé (Denton et al., 1999). North Patagonian rainforests with cold-resistant conifers (*Fitzroya-Pilgerodendron* and *Podocarpus*) were abundant until the Valdivian rainforest with thermophilous taxa developed and became dominant from ~11.5 to ~7.5 cal kyr BP, illustrating warmer and drier conditions in this region (e.g. Moreno and León, 2003; Abarzúa et al., 2004). The subsequent re-expansion of the North Patagonian rainforest taxa shows cooling events and precipitation increase during the mid- to late Holocene (Moreno, 2004).

This region also gave rise to numerous marine palaeostudies (e.g. Lamy et al., 2001, 2004; Kim et al., 2002; Kaiser et al., 2005, 2008; Mohtadi et al., 2008), however, comparing these marine and

continental records can produce discrepancies. The origins of these differences are difficult to associate with the age model applied and/or data interpretation. As it has been already shown in the northern hemisphere, pollen analysis from marine cores allows for comparison and correlation between marine and continental palaeorecords that can separate regional and local signals (e.g. Heusser and Balsam, 1977; Combourieu Nebout et al., 2002; Sánchez Goñi et al., 2002; Dupont and Wyputta, 2003; Hooghiemstra et al., 2006; Desprat et al., 2007). In southern Chile, past vegetation changes from marine cores have been poorly investigated except two sites in open ocean at $\sim 41^{\circ}\text{S}$ and 36°S (Heusser et al., 2006a, 2006b). These off-shore studies provided two continuous regional records of past vegetation illustrating the glacial/interglacial transition since 50 cal kyr BP that closely resemble changes in Antarctic ice core data. Here we report the first marine pollen record from a fjord in southern Chile from core MD07-3104 to reconstruct regional vegetation and climate changes from 13 cal kyr BP around Seno Reloncaví. Detailed comparisons with the numerous terrestrial pollen records of northwestern Patagonia will strengthen climatic reconstruction in this region and will help to discriminate local versus regional vegetation changes. In addition, this detailed comparison will provide support for the regional significance of marine and continental data sources and for the age model established in the studied core.

2. Environmental Setting

The seaway, "Seno Reloncaví" ($41^{\circ}20'$ - 42°S , Fig. 1B) is located in the Chilean Lake District. This region is characterized by numerous lakes resulting from glacial erosion that has hollowed out a central valley bordered by the "Cordillera de la Costa" to the west and the "Cordillera de los Andes" to the east. Frequent tectonic activity here results in numerous volcanoes along the "Cordillera de los Andes", and earthquakes trigger numerous landslides both on land, in lakes, and in fjords (St-Onge et al., 2012; Chapron et al., 2006).

In this region, the climate is temperate and hyper-humid. The precipitation is almost entirely controlled by the southern hemisphere westerly winds (Garreaud, 2007; Garreaud et al., 2009). During the austral winter, the northern margin of the westerly wind belt shifts northward, causing high rainfall in this region up to $\sim 30^{\circ}\text{S}$. During the austral summer, the westerly wind belt shifts south of 45°S . At Puerto Montt, the mean annual temperature at around 10°C is rather uniform throughout the year, however, precipitation shows strong seasonality and reaches around 2000 mm year⁻¹. Increasing altitude on the western flank of the Andes generates a high climatic gradient with strong orographic rainfall (3000 to 5000 mm) and a decrease in temperature such as at Lago Todos los Santos (Fig. 1C, data from New_LocClim software; Grieser et al., 2006).

Influenced by the prevailing westerly winds, the open ocean circulation is characterized by the Antarctic Circumpolar Current (ACC) that generates two surface currents (Fig. 1A): (i) an equatorward surface current called the Peru-Chile Current (PCC) flowing from 38°S in austral winter and from 45°S in austral summer and, (ii) a rather diffuse poleward surface current called the Cape Horn Current (CHC) that flows from 38°S in austral winter and from 46°S in austral summer (Strub et al., 1998). These currents follow the Pacific coast and have therefore less influence in the fjord system than in open ocean. In Seno Reloncaví, two main water masses are identified (Siever and Silva, 2008): (i) the Estuarine Water, a surface layer that moves from a fresh water source to the ocean and, (ii) the Subantarctic Water (>30 m depth), an intermediate layer modified by surface fresh water, enters by Golfo Corcovado and flows northward as far as Seno Reloncaví (Fig. 1A). The water masses are also influenced by tide and fluvial discharges that induce estuarine conditions due to the surface runoff, groundwater flows, and local rivers (Pantoja et al., 2011). For example, Petrohué River flows into the Reloncaví Fjord and generates a high river discharge of around $278 \text{ m}^3\text{s}^{-1}$ (Dirección General de Aguas, www.dga.cl).

The southern Chilean vegetation is characterized by seven main associations according to latitude and altitude (Fig. 1A). In the Chilean Lake District, the vegetation corresponds to a broadleaf temperate rainforest growing between 0 and 1200/1300 m above sea level (asl) including

several associations (e.g. Schimithüsen, 1956; Heusser, 1966; Villagrán, 1980; Moreno et al., 1999):

- Below ~500/600 m asl, the Valdivian rainforest predominates and shows high forest diversity with the development of numerous species of trees (Schimithüsen, 1956). The main characteristic species are *Nothofagus dombeyi*, *Eucryphia cordifolia*, *Aextoxicon punctatum*, *Caldcluvia paniculata*, and *Weinmannia trichosperma*. Woody climbers such as *Hydrangea serratifolia*, *Pseudopanax laetevirens* and epiphytic taxa such as *Misodendrum linearifolium* grow frequently in these forest communities.
- Between ~600 and ~1000 m asl, the North Patagonian rainforest predominates and is characterized by tree species such as *Nothofagus dombeyi*, *Nothofagus nitida*, *Nothofagus betuloides*, *Weinmannia trichosperma*, *Drimys winteri* and several species of Myrtaceae. This vegetation is associated with cold-resistant conifers such as *Fitzroya cupressoides*, *Pilgerodendron uviferum* and *Podocarpus nubigena*. The poorly drained sites result in the development of open forests with the predominance of *Pilgerodendron uviferum*, *Tepualia stipularis* and *Nothofagus nitida* (Haberle and Bennett, 2001).
- Between ~1000 and ~1200/1300 m asl, the North Patagonian rainforest is replaced by the Subantarctic deciduous forest, characterized by tree species *Nothofagus pumilio* and *Nothofagus antarctica*.
- The altitude 1200/1300 m asl corresponds to the tree-line above which the Andean tundra develops with open vegetation. The main representative plants are herbs or shrubs such as Asteraceae (*Baccharis* spp., *Nassauvia* spp.), Ericaceous shrubs (*Empetrum rubrum*, *Pernettya poepiggi*), *Astelia pumila*, *Drosera uniflora*, *Myrteola nummularia*, Apiaceae (*Azorella* spp.).

In southern Chile, a study has shown that the pollen input in marine surface sediment samples reflects the local vegetation from the nearby continental area (Montade et al., 2011). In Seno

Reloncaví, the pollen input can be explained by the combination of different transport mechanisms. In particular, the high river discharges in Seno Reloncaví, the major source of sediments, provide important terrigenous organic matter (Silva et al., 2011) including pollen. The irregular bottom topography and the presence of several sills slow down the water masses circulation and enhance the deposition and the sinking of particles (Siever and Silva, 2008; Pantoja et al., 2011). Therefore, the terrestrial material is largely retained within the fjords and decreases rapidly from the fjords to the open ocean (St-Onge et al., 2012; Aracena et al., 2011; Silva et al., 2011). These processes reduce the pollen drifting by currents in the Patagonian fjords such as in the Seno Reloncaví and reduce pollen degradation by oxidation, maximizing pollen preservation in the sediment. Pollen input is also reinforced by the contribution of the strong westerly winds that carry pollen from the surrounding lands to Seno Reloncaví (Montade et al., 2011). Consequently, this setting limits long distance pollen transport. Pollen content of core MD07-3104, mainly transported by high fluvial discharge and winds, represents the local to regional vegetation around Seno Reloncaví. These conditions explain the high pollen concentration values in Seno Reloncaví, which are among the highest values recorded in marine surface sediment samples of southern Chile (Fig. 4 and Montade et al., 2011). In addition, these high values are also reinforced by the high pollen productivity of evergreen rainforest trees in comparison with the open herbaceous/forest vegetation developed in southern Patagonia.

3. Materials and Methods

3.1. Lithology

Core MD07 3104 (41°42'40''S, 072°46'41''W, 326 m water depth, 21.77 m length) was taken in the main basin of Seno Reloncaví during the "PACHIDERME" cruise MD/159, on board of R/V Marion Dufresne II, with a CALYPSO Piston corer (Kissel and The Shipboard Scientific Party, 2007). In addition, a 7 m-long CALYPSO CASQ gravity corer (MD07-3105 Cq) was retrieved at a

nearby location to sample well-preserved material near the water-sediment interface. The coring site in Seno Reloncaví was selected in undisturbed sediment drift deposits based on high-resolution seismic profiling. The lithologies of these two overlapping cores consist of homogenous and slightly bioturbated diatom-rich olive grey to greyish silty clays and frequently contains shells and shell fragments (Fig. 2). Digital images of core lithologies were measured onboard on a Geotek multi-sensor track and highlight a 5 cm-thick dark sandy tephra layer with a sharp basal contact and a gradational upper limit documented at 19.35 m core depth.

3.2. Chronology

The age-depth model of core MD07-3104 is based on 22 radiocarbon dates (Fig. 2; Table 1) performed at Poznan radiocarbon laboratory (Poland) and at LMC14 laboratory (France). This chronology is based on (numerous) shells, shell debris and some (rare) woody debris by running the “CLAM” program (Blaauw, 2010) under the mathematical software “R” version 2.12.2. Radiocarbon ages were converted to calendar (cal) years (yr) BP using the IntCal09 calibration curve (Reimer et al., 2009). One shell and one woody fragment dated in core MD07-3105 Cq were integrated into the MD07-3104 age-depth model based on the precise correlation of sedimentary facies from both cores. In addition, one woody fragment and shell debris sampled at the same core depth in the nearby Calypso core MD07-3107 retrieved in Reloncaví fjord (cf. St-Onge et al., 2012) within bioturbated clays allowed estimation of the reservoir age (575 yr) that should be applied to radiocarbon dates on shells older than 5000 ^{14}C yr BP in this study area. This estimation seems to be supported in core MD07-3104 by correlating an outstanding black tephra layer occurring at 19.35 m core depth and dated to 11,106 \pm 136 cal yr BP with a major regional eruption. This tephra could be associated with the Volcán Chaitén dated at $\sim 9600 \pm 50$ ^{14}C yr BP (10,950 \pm 130 cal yr BP), as this has been suggested both in lacustrine cores as well as in the ODP site 1233 (Hajdas et al., 2003; Moreno and León, 2003; Abarzúa et al., 2004; Lamy et al., 2004; Abarzúa and

Moreno, 2008). However, no detailed geochemical analyses of this tephra in marine and terrestrial records were published, and this kind of study will be necessary to confirm the link between this tephra and the Volcán Chaitén. Based on the identification of several major historical earthquakes in core MD07-3107 from Reloncaví fjord, St-Onge et al. (2012) have also shown that a reservoir age of 400 yr should be applied to radiocarbon dates on shells younger than 5000 ^{14}C yr BP. Thus in core MD07-3104, a reservoir age of 400 yr was applied for the late Holocene and 575 yr for the Late Glacial and the early to mid-Holocene.

3.3. Pollen analysis

Pollen samples were prepared using the classical chemical protocol from Faegri and Iversen (1975): after drying, volume measuring, and sieving through a 150 μm mesh screen, pollen samples were treated using HCl and HF. A known amount of *Lycopodium* spores (in a calibrated tablet) were added to each sample prior to chemical treatment in order to calculate the pollen concentration (grains cm^{-3}) and pollen accumulation rates (grains $\text{cm}^{-2} \text{yr}^{-1}$). The residues were mounted on palynological slides with glycerin, and pollen grains were counted using a light microscope (Olympus BX51) at $\times 400$ magnification or $\times 1000$ magnification for determination. Several pollen atlases were used to aid pollen identification (Heusser, 1971; Markgraf and d' Antoni, 1978; Villagrán, 1980). Sample counts are ≥ 300 of pollen grains, and pollen percentages are based on sums of 62 pollen taxa determined in 57 pollen samples. Percentages were calculated on the total pollen sum (excluding unknown, spores and exotic pollen). Spore percentages were calculated on the total pollen sum (excluding unknown and exotic pollen). The pollen diagrams were plotted using Psimpoll (Bennett, 1994) and divided into zones based on a Constrained Cluster Analysis by Sum of Squares analysis (CONISS) with pollen taxa $\geq 1\%$ (Grimm, 1987). Principal Component Analysis (PCA) was performed on pollen taxa $\geq 5\%$. PCA represents two dimensional-plots or biplots between pollen taxa and each pollen sample.

4. Results

4.1. Pollen zones

The MD07-3104 pollen records are presented in percentages and concentrations (Figs. 3, 4 and 5). The pollen diagram is divided into 7 pollen zones showing the major changes of key indicator taxa presented in Table 2. The total pollen concentrations are very high and fluctuate between 10,000 and 45,000 grains cm^{-3} (Fig. 4). Several concentration peaks show a millennial variability with regular intervals of ~1000/2000 kyr at around 2.2 (215 cm), 2.9 (445 cm), 4.8 (815 cm), 7.1 (1045 cm), 8.7 (1225 cm), 9.6 (1605 cm), 10.8 (1905 cm) and 12.1 cal kyr BP (2095 cm). However, this millennial variability requires higher temporal resolution in order to be confirmed. These peaks also occur in pollen accumulation rates in different proportions due to the sedimentation rate changes. This could reflect changes of sediment inputs or pollen preservation; however it is difficult to discriminate the main factor. Different taxa are associated with these peaks according to the depth (Fig. 4) and therefore, these peaks have probably not influenced the general picture of the vegetation changes.

4.2. Principal Component Analysis

PCA is used to reduce the pollen data into a two-dimensional plot, with the resulting data set displayed as a biplot for samples and taxa. Fig. 5a plots the eigenvectors for the main pollen taxa according to these two axes. The horizontal axis 1 mainly contrasts *Hydrangea*, *Eucryphia-Caldcluvia*, Myrtaceae, Poaceae, and *Nothofagus dombeyi* type with *Podocarpus*, *Fitzroya-Pilgerodendron* and the ubiquitous taxon *Weinmannia*. The Valdivian rainforest taxa (*Hydrangea*, *Eucryphia-Caldcluvia*, Myrtaceae) and the *Nothofagus*-Poaceae association grow generally under drier conditions than the conifer taxa (*Podocarpus* and *Fitzroya-Pilgerodendron*) and the ubiquitous

taxon *Weinmannia*. Consequently, this first axis seems to oppose drier (negative values) versus wetter (positive values) conditions. The vertical axis 2 contrasts *Nothofagus dombeyi* type, *Misodendrum*, *Podocarpus*, *Fitzroya-Pilgerodendron*, and Poaceae with *Aextoxicon-Escallonia*, *Weinmannia*, *Hydrangea*, and Myrtaceae. The cold-resistant conifer taxa (*Podocarpus* and *Fitzroya-Pilgerodendron*), *Nothofagus dombeyi* type and Poaceae can grow under cooler conditions than the other taxa. This second axis seems to be related to temperature and opposes the North Patagonian rainforest taxa living under cooler conditions (negative values) versus the Valdivian rainforest taxa living under warmer conditions (positive values). *Misodendrum* is plotted near *Nothofagus dombeyi* type, because it is a parasite of *Nothofagus* trees. Fig. 5b plots samples eigenvalues according to the 7 pollen zones that reflect the succession of vegetation changes during the last 13 cal kyr BP.

5. Palaeoenvironment reconstruction from core MD07-3104

The 7 pollen zones from core MD07-3104 highlight the pollen percentage changes related to vegetation changes around the Seno Reloncaví (Table 2, Fig. 3). The percentages dominated by the arboreal pollen (between 78 and 90%, Fig. 3) suggest a significant development and a continuous presence of the closed canopy rainforest since 13 cal kyr BP.

Before 12.3 cal kyr BP (SR-1, 2115-2172 cm), high frequencies of cold resistant-conifer taxa, such as *Fitzroya-Pilgerodendron* and *Podocarpus* (probably *P. nubigena*), are recorded and are associated with *Nothofagus dombeyi* type and Myrtaceae. Pollen analysis of surface sediment has shown that such an association grows under cooler and wetter conditions in the North Patagonian rainforest from mid- to high-elevation (Paez et al., 1997) or southward in the region of Chonos Archipelago (Haberle and Bennett, 2001). Thus, these results suggest a low temperature and high precipitation regime during this first pollen zone.

From 12.3 to 10.7 cal kyr BP (SR-2, 1885-2115 cm), *Weinmannia* (*W. trichosperma*) increases abruptly. *Weinmannia* is a shade-intolerant tree that grows today in the Valdivian and North Patagonian rainforest (Villagrán, 1993). This tree species expands in forest affected by high disturbance such as climate changes, fire, or anthropogenic influences (e.g. Veblen et al., 1980; Donoso, 1993; Villagrán, 1993; Lusk, 1999). The spread in *Weinmannia* in core MD07-3104 thus marks the decline of North Patagonian rainforest taxa around Seno Reloncaví. However, it is difficult to determine whether climate change and/or local disturbances such as fire activity, edaphic changes, or opening of the forest canopy was the principal cause of *Weinmannia* increase. A volcanic eruption occurred at 11.1 cal kyr BP (19.35 m depth) during this pollen zone and has probably generated disturbances. However this eruption occurred after the onset of the *Weinmannia*-dominated woodland and cannot be therefore the primary factor of the *Weinmannia* expansion.

At 10.7 cal kyr BP (SR-3, 1585-1885 cm), *Weinmannia* declines abruptly. Simultaneously, thermophilous taxa expand mainly with *Eucryphia-Caldcluvia* and *Aextoxicon-Escallonia*. With low presence of cold-resistant conifers, these vegetation changes illustrate the expansion of the Valdivian rainforest under warmer and drier conditions than the North Patagonian rainforest and mark the beginning of the Holocene. This trend is strengthened between 9.6 and 7.4 cal kyr BP (SR-4, 1060-1585 cm) with continuous expansion of *Eucryphia-Caldcluvia*. Axes 1 and 2 of the PCA (Fig. 6) also illustrate this trend and show changes toward warmer and drier conditions from 10.7 to 7.4 cal kyr BP (SR-3 to SR-4).

Between 7.4 and 6.7 cal kyr BP (SR-5, 1025-1060 cm), *Nothofagus dombeyi* type expanded abruptly with a slight development of *Podocarpus* and Poaceae and a decline of all other taxa. The thermophilous taxa decrease interrupts the warming trend and marks the end of the Holocene Climatic Optimum.

Between 6.7 and 2.8 cal kyr BP (SR-6, 425-1025 cm), the shade-intolerant tree *Weinmannia*, related to a forest disturbance, re-expands. *Nothofagus dombeyi* type, anti-correlated with pulses of

Eucryphia-Caldcluvia, highlights a rapid alternation between cool and warm phases. Then, after ~6-5 cal kyr BP, *Fitzroya-Pilgerodendron* shows a progressive increase and underlines a progressive increase of humid conditions. The PCA polygon SR-6 appears poorly defined because it is superimposed over the other polygons (SR-7/4). This shows the increase in variability of vegetation changes probably linked to an increase of climate variability (Fig. 5). The PCA axis 2 values shift toward cooler conditions during SR-5 while the PCA axis 1 values shift toward wetter conditions later in the following pollen zone SR-6 after ~6-5 cal kyr BP (Fig. 6). This suggests a short time lag between temperature changes and the precipitation decrease after the Holocene Climatic Optimum. After 2.8 cal kyr BP (SR-7, 5-425 cm), the cold-resistant conifers (*Fitzroya-Pilgerodendron* and *Podocarpus*) and *Nothofagus dombeyi* type expand while *Weinmannia* and *Eucryphia-Caldcluvia* progressively decline. Such a change shows an expansion of North Patagonian rainforest taxa. This marks a gradual cooling trend with an increase of precipitation. The axis 1 and 2 of PCA highlight this climate change toward cooler and wetter conditions (Fig. 6) and the SR-7 polygon is partly superimposed to the SR-1 polygon due to the high percentages of the cold-resistant conifers in these two pollen zones (Fig. 5).

6. Comparison with regional records

The comparison of marine pollen results from core MD07-3104 with continental pollen results around Seno Reloncaví permits to discriminate the difference between these two kinds of records and to improve the regional picture of vegetation and climate changes. Before 11.5-12 cal kyr BP, cool and wet conditions are illustrated by the development of the North Patagonian rainforest in core MD07-3104 (Fig. 7). These conditions, also recorded at the Huelmo site (Moreno and León, 2003) and Lago Condorito (Moreno, 2004), represent the end of the Last Glacial-Interglacial Transition synchronous with the end of the Huelmo-Mascardi Cold Reversal between ~13.5 and 11.5 cal kyr BP (Ariztegui et al., 1997; Moreno et al., 2001; Hajdas et al., 2003). At 12.3 cal kyr

BP, the abrupt expansion of *Weinmannia* recorded in core MD07-3104 corresponds roughly with the expansion of *Weinmannia* observed in the terrestrial pollen records, varying from site to site: 12.9 cal kyr BP at the Huelmo site (Moreno and León, 2003), 12.5 cal kyr BP at Lago Condorito (Moreno, 2004), ~11.5 cal kyr BP at the Alerce site (Heusser, 1966), 11.7 cal kyr BP at Laguna Melli (Abarzúa and Moreno, 2008) and 11.5 cal kyr BP at Laguna Tahui (Abarzúa et al., 2004). At around 12 cal kyr BP at nearly all sites south of latitude 40°S, the fire activity increased, illustrating the warmer conditions and increased aridity (e.g. Moreno, 2000; Haberle and Bennett, 2004; Whitlock et al., 2007; Abarzúa and Moreno, 2008). This regional expansion of *Weinmannia*-dominated woodlands in northern Patagonia could be thus linked to this climate change and/or to the regional increase of fire activity.

In core MD07-3104, the early Holocene, beginning at 10.7 cal kyr BP, corresponds to the expansion of Valdivian rainforest taxa illustrating the warmest and driest conditions of the Holocene between 9.6 and 7.4 cal kyr BP. This period marks the Holocene Climatic Optimum also recorded at Lago Condorito (Fig. 7) between 10 and 7.6 cal kyr BP (Moreno, 2004) and at the Alerce site between ~10 and ~7 cal kyr BP (Heusser, 1966).

After 7.4 cal kyr BP, the abrupt development of *Nothofagus* trees is only recorded in one sample; however, this change in *Nothofagus* composition is also observed in Lago Condorito around 7.6 cal kyr BP (Moreno, 2004). From 7.4 to 2.8 cal kyr BP, the vegetation shows high variability, illustrating recurrent cooling in pulses with an increase in precipitation after ~6-5 cal kyr BP. Such a climatic instability during the mid-Holocene is also evidenced in terrestrial sites around Seno Reloncaví at the Alerce (Heusser, 1966) and Lago Condorito sites (Fig. 7) with several repetitive expansions of the North Patagonian rainforest. Nevertheless the timing of the rapid cooling events that are recorded at 6.9, 5.7 and 4.5 cal kyr BP in Lago Codorito (Moreno, 2004) remain imprecise in the vegetation record of core MD07-3104, as the sampling resolution is still too low for such interpretations during the mid-Holocene.

After 2.8 cal kyr BP, the expansion of the North Patagonian rainforest recorded in MD07-3104 shows the increase of cool and wet conditions that persist until the present. Such a change differs slightly from the Lago Condorito pollen record, showing a slight decline in North Patagonian forest after 2.9 cal kyr BP (Moreno, 2004). However, cool and moist conditions were already observed during the late Holocene at the Alerce site (Heusser, 1966), Lago Puyehue (Vargas-Ramirez et al., 2008), Laguna Tahui (Abarzúa et al., 2004) and the Vicente Pérez Rosales National Park (Villagrán, 1980). As suggested by Heusser (1966), the decline of thermophilous taxa that generally grow in the lowland was probably reinforced by deforestation during the last centuries, especially after Spanish conquest around 1550-1600 A.D.

Despite a recurrent time lag observed in pollen zones between the marine and terrestrial pollen results in Fig. 7 (300 yr at ~13-10 cal kyr BP, 200 yr at ~8-7 cal kyr BP and 100 yr at ~3 cal kyr BP), this regional comparison illustrates that the timing and the trend of vegetation/climate changes from core MD07-3104 are correlated with those recorded at terrestrial sites around Seno Reloncaví. This recurrent time lag could be the result of underestimated reservoir ages that change from the beginning to the end of the Holocene. However, the temporal resolution of the marine pollen analyses (~200 yr) precludes confirmation of this hypothesis or a link to the error interval of the radiocarbon ages. Compared to the terrestrial pollen records, marine pollen analyses show a continuous presence of several taxa that can be missing or represented in very low percentages in terrestrial sites during some periods. For example, the cold-resistant conifers, such as *Podocarpus* or *Fitzroya-Pilgerodendron*, are near zero in terrestrial sites between ~11 and ~7 cal kyr BP (e.g. Abarzúa et al., 2004; Moreno, 2004), however, they are still present in the marine pollen record with low percentage values. The marine pollen data illustrate therefore a more regional vegetation and climate signal around Seno Reloncaví, likely due to a larger sediment input.

7. Conclusion

The palynological data from core MD07-3104 provide the first marine pollen record from a southern Chilean fjord around Seno Reloncaví and illustrate the vegetation and climate changes during the last ~13 cal kyr BP:

- The marine pollen data illustrate cool and wet condition before ~11.5-12 cal kyr BP with the presence of cold-resistant conifers (*Fitzroya-Pilgerodendron* and *Podocarpus*) during the end of Termination I.
- After that, the development of *Weinmannia* marks a climate change probably under warming conditions and with high rates of disturbance. This trend is strengthened at 10.7 cal kyr BP by the increase of heliophytic taxa (*Eucryphia-Caldcluvia*). The heliophytic taxa reach their maximum expansion between 9.6 and 7.4 cal kyr BP, during the Holocene Climatic Optimum with warm and dry conditions.
- After 7.4 cal kyr BP, the mid-Holocene is characterized by an increase in climate variability associated with a cooling trend and an increase in precipitation that seems to occur after 6-5 cal kyr BP.
- The cooler and wetter conditions are strengthened during the late Holocene after 2.8 cal kyr BP with the expansion of cold-resistant conifer taxa.

The pollen record from core MD07-3104 is correlated with the terrestrial pollen records of northwestern Patagonia. These records illustrate the same trends and the close timing of vegetation/climate changes, supporting changes in southern westerly wind intensity and/or position in northern Patagonia during the Holocene. In comparison to the terrestrial pollen records, this marine pollen record provides a regional signal of vegetation/climate changes and clearly demonstrates the sensitivity of marine pollen records to reconstruct such changes in this region. The sedimentation input variation during the last 13 cal kyr BP does not modify the general picture of vegetation changes in core MD07-3104, and the pollen input remains thus local to regional in scale at Seno Reloncaví. Despite the slight time lags between marine and continental pollen records, the close timing of vegetation changes support the age model established in the studied core. A more

refined temporal resolution of marine pollen analysis seems to be an interesting research perspective to better study the variations of marine reservoir ages and to confirm the rapid climatic events already recorded in terrestrial pollen results from the mid- to late Holocene in this region. In addition, this kind of study may be interesting to develop further in other Chilean fjords, especially in the regions difficult to access by land.

Acknowledgements

This research was supported by the Laboratoire des Sciences du Climat et de l'Environnement (LSCE), the Centre National de la Recherche Scientifique, the Commissariat à l'Energie Atomique, the Université Versailles St Quentin and the Université Paris Sud 11. We would like to thank the Institut Polaire Français Paul Emile Victor and the shipboard scientific party for the MD159/PACHIDERME cruise that collected the core material and data on board of the French vessel "*Marion Dufresne II*". We thank M. H. Castera and J. L. Turon for the chemical treatment and S. Ivory for its very helpful comments. Radiocarbon dating in this study was performed at Poznan radiocarbon laboratory (Poland) and LMC14 laboratory in Saclay (France), thanks to the French national program ARTEMIS from INSU. We are also grateful for the very constructive comments from P.I. Moreno and one anonymous referee in improving this paper.

References

- Abarzúa, A.M., Moreno, P.I., 2008. Changing fire regimes in the temperate rainforest region of southern Chile over the last 16,000 yr. *Quaternary. Res.* 69, 62-71.
- Abarzúa, A.M., Villagrán, C., Moreno, P.I., 2004. Deglacial and postglacial climate history in east-central Isla Grande de Chiloé, southern Chile (43°S). *Quaternary. Res.* 62, 49-59.
- Aracena, C., Lange, C.B., Luis Iriarte, J., Rebolledo, L., Pantoja, S., 2011. Latitudinal patterns of export production recorded in surface sediments of the Chilean Patagonian fjords (41-55°S) as a response to water column productivity. *Cont. Shelf. Res.* 31, 340-355.
- Ariztegui, D., Bianchi, M.M., Massafiero, J., Lafargue, E., Niessen, F., 1997. Interhemispheric synchrony of Late-glacial climatic instability as recorded in proglacial Lake Mascardi, Argentina. *J. Quaternary Sci.* 12, 333-338.
- Bennett, K.D., 1994. "psimpoll" version 2.23: a C program for analysing pollen data and plotting pollen diagrams. INQUA Commission for the study of the Holocene: Working group on data-handling methods, Newsletter 11, 4-6.
- Blaauw, M., 2010. Methods and code for classical age-modelling of radiocarbon sequences. *Quaternary Geochronology* 5, 512-518.
- Chapron, E., Ariztegui, D., Mulsow, S., Villarosa, G., Pino, M., Outes, V., Juvignié, E., Crivelli, E., 2006. Impact of the 1960 major subduction earthquake in Northern Patagonia (Chile, Argentina). *Quatern. Int.* 158, 58-71.
- Combourieu Nebout, N., Peyron, O., Dormoy, I., Desprat, S., Beaudouin, C., Kotthoff, U., Marret, F., 2009. Rapid climatic variability in the west Mediterranean during the last 25 000 years from high resolution pollen data. *Clim. Past* 5, 503-521.
- Denton, G.H., Lowell, T.V., Heusser, C.J., Schluchter, C., Andersen, B.G., Heusser, L.E., Moreno, P.I., Marchant, D.R., 1999. Geomorphology, Stratigraphy, and Radiocarbon Chronology of

- Llanquihue Drift in the Area of the Southern Lake District, Seno Reloncavi, and Isla Grande de Chiloe, Chile. *Geogr. Ann. A* 81, 167-229.
- Desprat, S., Sánchez Goñi, M.F., Naughton, F., Turon, J.-L., Duprat, J., Malaizé, B., Cortijo, E., Peyrouquet, J.-P., 2007. 25. Climate variability of the last five isotopic interglacials: Direct land-sea-ice correlation from the multiproxy analysis of North-Western Iberian margin deep-sea cores, in: *The Climate of Past Interglacials*. Elsevier, pp. 375–386.
- Donoso, C., 1993. Bosques Templados de Chile y Argentina, Variación, Estructura, y Dinámica. *Boletín técnico Facultad de Ciencias Forestales, Universidad de Chile* 54, 1-27.
- Dupont, L.M., Wyputta, U., 2003. Reconstructing pathways of aeolian pollen transport to the marine sediments along the coastline of SW Africa. *Quaternary Sci. Rev.* 22, 157–174.
- Fægri, K., Iversen, J., 1975. *Textbook of Pollen Analysis*, John Wiley & Sons. ed. London.
- Garreaud, R.D., 2007. Precipitation and Circulation Covariability in the Extratropics. *J. Climate* 20, 4789-4797.
- Garreaud, R.D., Vuille, M., Compagnucci, R., Marengo, J., 2009. Present-day South American climate. *Palaeogeogr. Palaeoclimatol.* 281, 180-195.
- Grieser, J., Girommes, R., Bernardi, M., 2006. New_LocClim - the Local Climate Estimator of FAO. *Geophysical Research Abstracts* 8, 08305.
- Grimm, E., 1987. CONISS: a FORTRAN 77 program for stratigraphically constrained cluster analysis by the method of incremental sum of squares. *Comput. Geosci.* 13, 13-35.
- Haberle, S.G., Bennett, K.D., 2001. Modern pollen rain and lake mud-water interface geochemistry along environmental gradients in southern Chile. *Rev. Palaeobot. Palynol.* 117, 93-107.
- Haberle, S.G., Bennett, K.D., 2004. Postglacial formation and dynamics of North Patagonian Rainforest in the Chonos Archipelago, Southern Chile. *Quaternary Sci. Rev.* 23, 2433-2452.
- Hajdas, I., Bonani, G., Moreno, P.I., Ariztegui, D., 2003. Precise radiocarbon dating of Late-Glacial cooling in mid-latitude South America. *Quaternary Res.* 59, 70-78.

- Heusser, C.J., 1966. Late-Pleistocene Pollen Diagrams from the Province of Llanquihue, Southern Chile. *P. Am. Philos. Soc.* 110, 269-305.
- Heusser, C.J., 1971. *Pollen and Spores of Chile*, The University of Arizona Press. ed. Tuscon, Arizona.
- Heusser, C.J., Lowell, T.V., Heusser, L.E., Hauser, A., Andersen, B.G., Denton, G.H., 1996. Full-glacial-late-glacial palaeoclimate of the southern Andes: evidence from the pollen, beetle and glacial records. *J. Quaternary Sci.* 11, 173-184.
- Heusser, C.J., Streeter, S.S., Stuiver, M., 1981. Temperature and precipitation record in southern Chile extended to ~ 43,000 yr ago. *Nature* 294, 65-67.
- Heusser, L., Balsam, W.L., 1977. Pollen distribution in the northeast Pacific Ocean. *Quaternary Res.* 7, 45–62.
- Heusser, L., Heusser, C., Mix, A., McManus, J., 2006a. Chilean and Southeast Pacific paleoclimate variations during the last glacial cycle: directly correlated pollen and $\delta^{18}\text{O}$ records from ODP Site 1234. *Quaternary Sci. Rev.* 25, 3404-3415.
- Heusser, L., Heusser, C., Pisias, N., 2006b. Vegetation and climate dynamics of southern Chile during the past 50,000 years: results of ODP Site 1233 pollen analysis. *Quaternary Sci. Rev.* 25, 474-485.
- Hooghiemstra, H., Lézine, A.-M., Leroy, S.A.G., Dupont, L., Marret, F., 2006. Late Quaternary palynology in marine sediments: A synthesis of the understanding of pollen distribution patterns in the NW African setting. *Quatern. Int.* 148, 29–44.
- IPCC, 2007. *Climate change 2007: the physical science basis: contribution of Working Group I to the Fourth Assessment Report of the Intergovernmental Panel on Climate Change*, Cambridge University Press. ed. Cambridge, United Kingdom and New York, USA.
- Kaiser, J., Lamy, F., Hebbeln, D., 2005. A 70-kyr sea surface temperature record of southern Chile (Ocean Drilling Program Site 1233). *Paleoceanography* 20, 1–15.

- Kaiser, J., Schefuß, E., Lamy, F., Mohtadi, M., Hebbeln, D., 2008. Glacial to Holocene changes in sea surface temperature and coastal vegetation in north central Chile: high versus low latitude forcing. *Quaternary Sci. Rev.* 27, 2064–2075.
- Kim, J.-H., Schneider, R., Hebbeln, D., Müller, P.J., Wefer, G., 2002. Last deglacial sea-surface temperature evolution in the Southeast Pacific compared to climate changes on the South America continent. *Quaternary Sci. Rev.* 21, 2085–2097.
- Kalnay, E., Kanamitsu, M., Kistler, R., Collins, W., Deaven, D., Gandin, L., Iredell, M., Saha, S., White, G., Woollen, J., Zhu, Y., Leetmaa, A., Reynolds, R., Chelliah, M., Ebisuzaki, W., Higgins, W., Janowiak, J., Mo, K.C., Ropelewski, C., Wang, J., Jenne, R., Joseph, D., 1996. The NCEP/NCAR 40-Year Reanalysis Project. *Bull. Amer. Meteor. Soc.* 77, 437-471.
- Kissel, C., The Shipboard Scientific Party, 2007. MD159-PACHIDERME-IMAGES XV, Cruise report, Les rapports de campagne à la mer, Réf. OCE/2007/01, Institut Paul- Emile Victor. ed.
- Lamy, F., Hebbeln, D., Röhl, U., Wefer, G., 2001. Holocene rainfall variability in southern Chile: a marine record of latitudinal shifts of the Southern Westerlies. *Earth Planet. Sc. Lett.* 185, 369–382.
- Lamy, F., Kaiser, J., Ninnemann, U., Hebbeln, D., Arz, H.W., Stoner, J., 2004. Antarctic Timing of Surface Water Changes off Chile and Patagonian Ice Sheet Response. *Science* 304, 1959-1962.
- Lusk, C.H., 1999. Long-lived light-demanding emergents in southern temperate forests: the case of *Weinmannia trichosperma* (Cunoniaceae) in Chile. *Plant. Ecol.* 140, 111–115.
- Markgraf, V., d' Antoni, H.L., 1978. Pollen Flora of Argentina, The University of Arizona Press. ed. Tucson, Arizona.
- Markgraf, V., Webb, R.S., Anderson, K.H., Anderson, L., 2002. Modern pollen/climate calibration for southern South America. *Palaeogeogr. Palaeoclimatol.* 181, 375-397.

- Montade, V., Nebout, N.C., Kissel, C., Mulsow, S., 2011. Pollen distribution in marine surface sediments from Chilean Patagonia. *Mar. Geol.* 282, 161-168.
- Moreno, P.I., 1997. Vegetation and climate near Lago Llanquihue in the Chilean Lake District between 20200 and 9500 14C yr BP. *J. Quaternary Sci.* 12, 485-500.
- Moreno, P.I., 2000. Climate, Fire, and Vegetation between About 13,000 and 9200 14C yr B.P. in the Chilean Lake District. *Quaternary Res.* 54, 81-89.
- Moreno, P.I., 2004. Millennial-scale climate variability in northwest Patagonia over the last 15 000 yr. *J. Quaternary Sci.* 19, 35-47.
- Moreno, P.I., Jacobson, G.L., Lowell, T.V., Denton, G.H., 2001. Interhemispheric climate links revealed by a late-glacial cooling episode in southern Chile. *Nature* 409, 804-808.
- Moreno, P.I., León, A.L., 2003. Abrupt vegetation changes during the last glacial to Holocene transition in mid-latitude South America. *J. Quaternary Sci.* 18, 787-800.
- Moreno, P.I., Lowell, T.V., George L. Jacobson Jr., Denton, G.H., 1999. Abrupt Vegetation and Climate Changes during the Last Glacial Maximum and Last Termination in the Chilean Lake District: A Case Study from Canal de la Puntilla (41°S). *Geogr. Ann. A* 81, 285-311.
- Mohtadi, M., Rossel, P., Lange, C.B., Pantoja, S., Böning, P., Repeta, D.J., Grunwald, M., Lamy, F., Hebbeln, D., Brumsack, H.-J., 2008. Deglacial pattern of circulation and marine productivity in the upwelling region off central-south Chile. *Earth Planet. Sc. Lett.* 221–230.
- Paez, M.M., Villagrán, C., Stutz, S., Hinojosa, F., Villa, R., 1997. Vegetation and pollen dispersal in the subtropical-temperate climatic transition of Chile and Argentina. *Rev. Palaeobot. Palyno.* 96, 169-181.
- Pantoja, S., Luis Iriarte, J., Daneri, G., 2011. Oceanography of the Chilean Patagonia. *Cont. Shelf. Res.* 31, 149-153.
- Reimer, P.J., Baillie, M.G.L., Bard, E., Bayliss, A., Beck, J.W., Blackwell, P.G., Ramsey, C.B., Buck, C.E., Burr, G.S., Edwards, R.L., Friedrich, M., Grootes, P.M., Guilderson, T.P., Hajdas, I., Heaton, T.J., Hogg, A.G., Hughen, K.A., Kaiser, K.F., Kromer, B., McCormac,

- F.G., Manning, S.W., Reimer, R.W., Richards, D.A., Southon, J.R., Talamo, S., Turney, C.S.M., van der Plicht, J., Weyhenmeyer, C.E., 2009. Intcal09 and Marine09 Radiocarbon Age Calibration Curves, 0-50,000 Years Cal Bp. *Radiocarbon* 51, 1111-1150.
- Sánchez Goñi, M.F., Cacho, I., Turon, J.-L., Guiot, J., Sierro, F., Peyrouquet, J.-P., Grimalt, J., Shackleton, N., 2002. Synchronicity between marine and terrestrial responses to millennial scale climatic variability during the last glacial period in the Mediterranean region. *Clim. Dynam.* 19, 95–105.
- Schimithüsen, J., 1956. Die räumliche Ordnung der chilenischen Vegetation. *Bonner Geographische Abhandlungen* 17, 1-86.
- Siever, A.H., Silva, N., 2008. Water masses and circulation in austral Chilean channels and fjords, in: Silva, N., Palma, S. (Eds.), *Progress in the Oceanographic Knowledge of Chilean Inner Waters, from Puerto Montt to Cape Horn*. Valparaíso, pp. 53-58.
- Silva, N., Vargas, C.A., Prego, R., 2011. Land-ocean distribution of allochthonous organic matter in surface sediments of the Chiloé and Aysén interior seas (Chilean Northern Patagonia). *Cont. Shelf. Res.* 31, 330-339.
- St-Onge, G., Chapron, E., Mulsow, S., Salas, M., Viel, M., Debret, M., Foucher, A., Mulder, T., Winiarski, T., Desmet, M., Costa, P.J.M., Ghaleb, B., Jaouen, A., Locat, J., 2012. Comparison of earthquake-triggered turbidites from the Saguenay (Eastern Canada) and Reloncavi (Chilean margin) Fjords: Implications for paleoseismicity and sedimentology. *Sediment. Geol.* 243–244, 89–107.
- Strub, P.T., Mesias, J.M., Montecio, V., Ruttlant, J., Salinas, S., 1998. Coastal ocean circulation off western South America.
- Vargas-Ramirez, L., Roche, E., Philippe, G., Hooghiemstra, H., 2008. A pollen-based record of late glacial holocene climatic variability in the southern lake district, Chile. *J. Paleolimnol.* 39, 197-217.

- Veblen, T.T., Schlegel, F.M., R., B.E., 1980. Structure and Dynamics of Old-Growth Nothofagus Forests in the Valdivian Andes, Chile. *J. Ecol.* 68, 1-31.
- Villagrán, C., 1980. Vegetationsgeschichtliche und pflanzensoziologische Untersuchungen im Vicente Perez Rosales Nationalpark Chile. *Dissertationes Botanicae* 54, 1-165.
- Villagrán, C., 1988a. Expansion of Magellanic Moorland during the late Pleistocene: Palynological evidence from northern Isla de Chiloé, Chile. *Quaternary Res.* 30, 304-314.
- Villagrán, C., 1988b. Late quaternary vegetation of southern Isla Grande de Chiloé, Chile. *Quaternary Res.* 29, 294-306.
- Villagrán, C., 1993. Glacial, late-glacial and postglacial climate and vegetation on Isla Grande de Chiloé, southern Chile (41-44°S). *Quaternary South America and Antarctic Peninsula* 8, 1-15.
- Whitlock, C., Moreno, P.I., Bartlein, P., 2007. Climatic controls of Holocene fire patterns in southern South America. *Quaternary Res.* 68, 28-36.

Figure captions

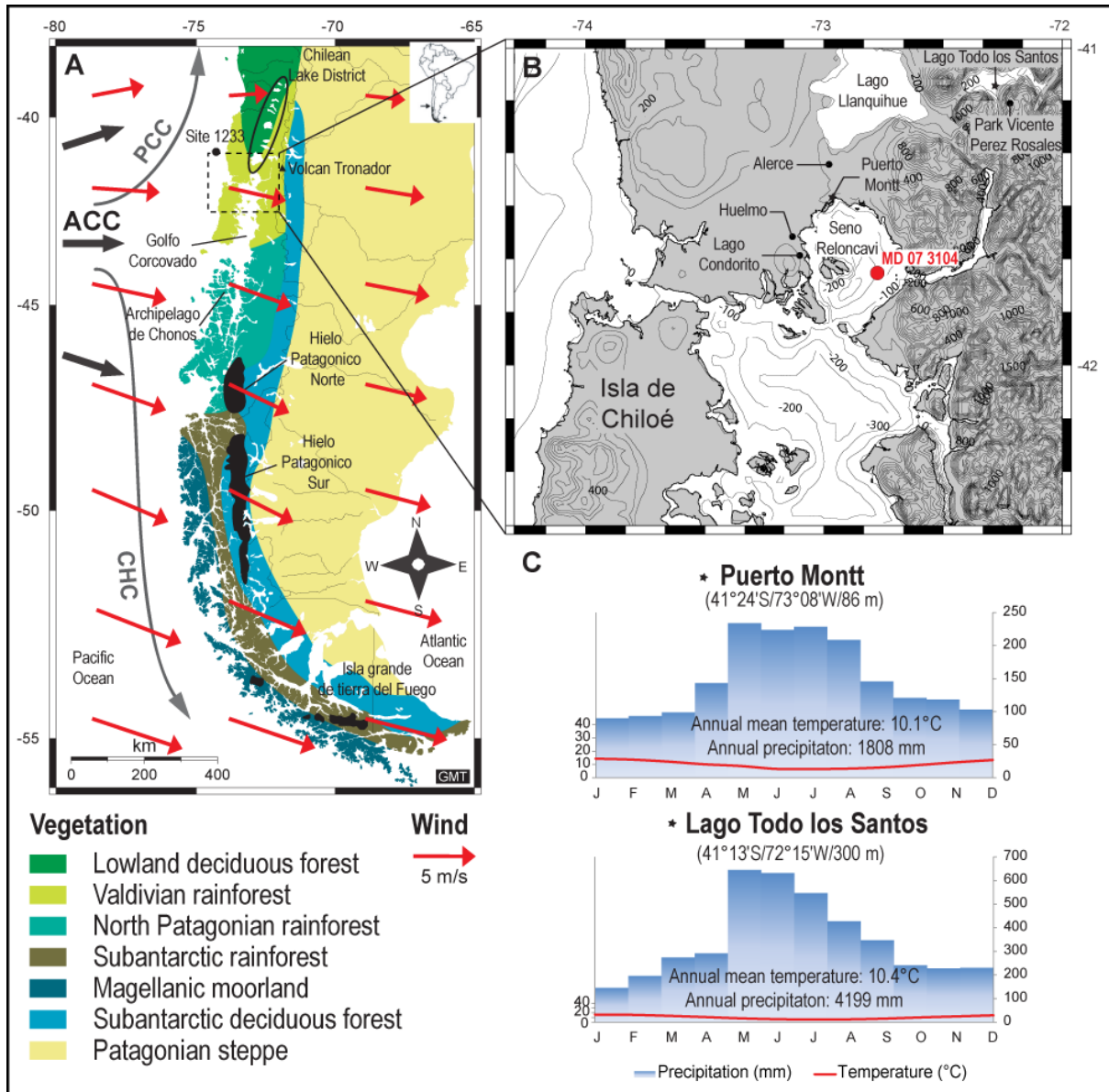


Fig. 1: Location maps of Patagonia and the study area: (A) Vegetation map (after Schimithüsen, 1956) with the southern Patagonian icefield (black area), annual average winds (Kalnay et al., 1996), and main oceanic currents (ACC, Antarctic Circumpolar Current, PCC, Peru Chile Current, CHC, Cape Horn Current) (Strub et al., 1998). (B) Location of core MD07-3104 in Seno Reloncaví and the main site discussed in the text. (C) Ombrothermic diagrams near the studied site (data from New_LocClim software; Grieser et al., 2006). On these diagrams, the precipitation scale is double the temperature scale, as is generally done for the ombrothermic diagrams.

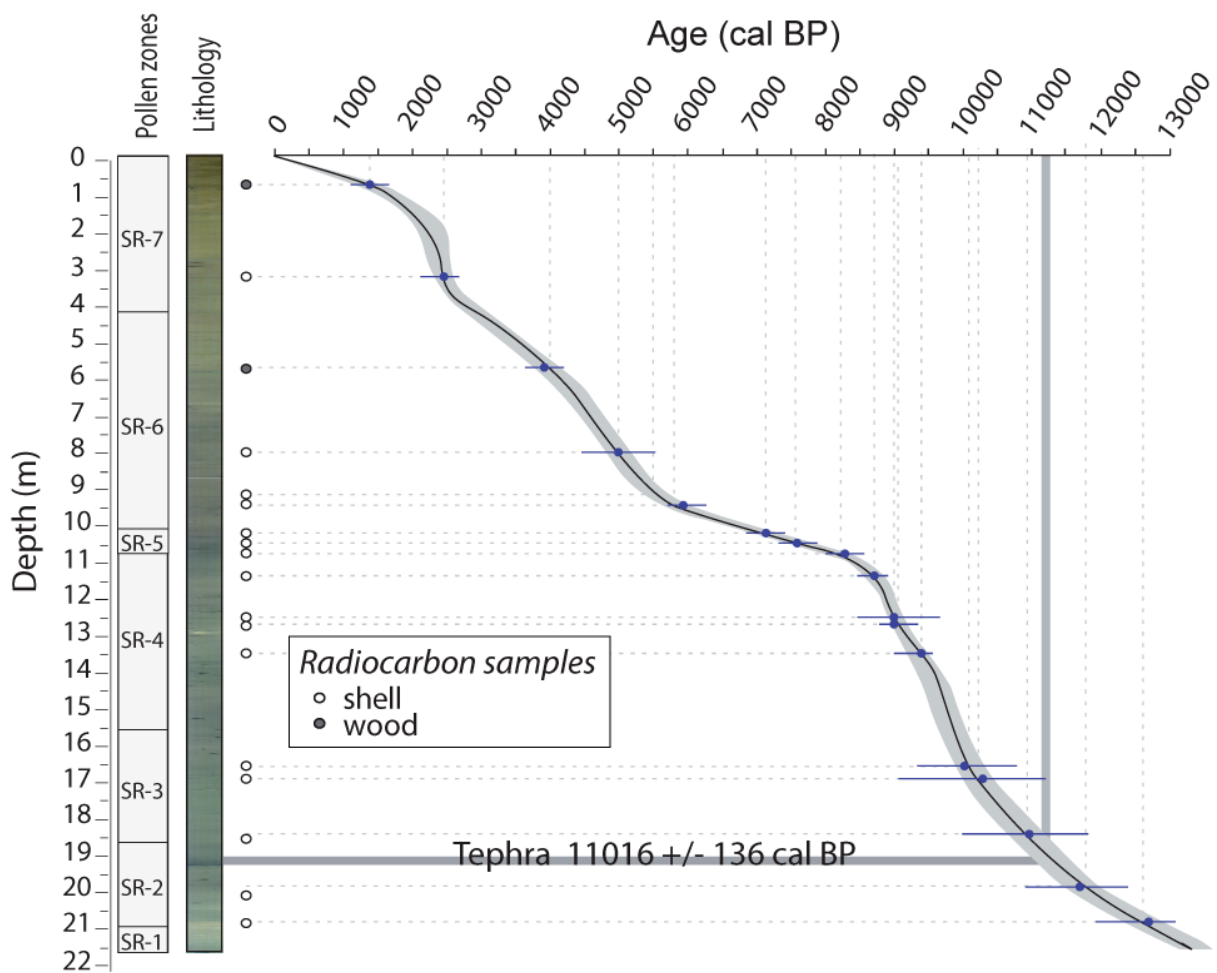


Fig. 2: Lithology, chronology, and pollen zones of core MD07-3104 in Seno Reloncaví.

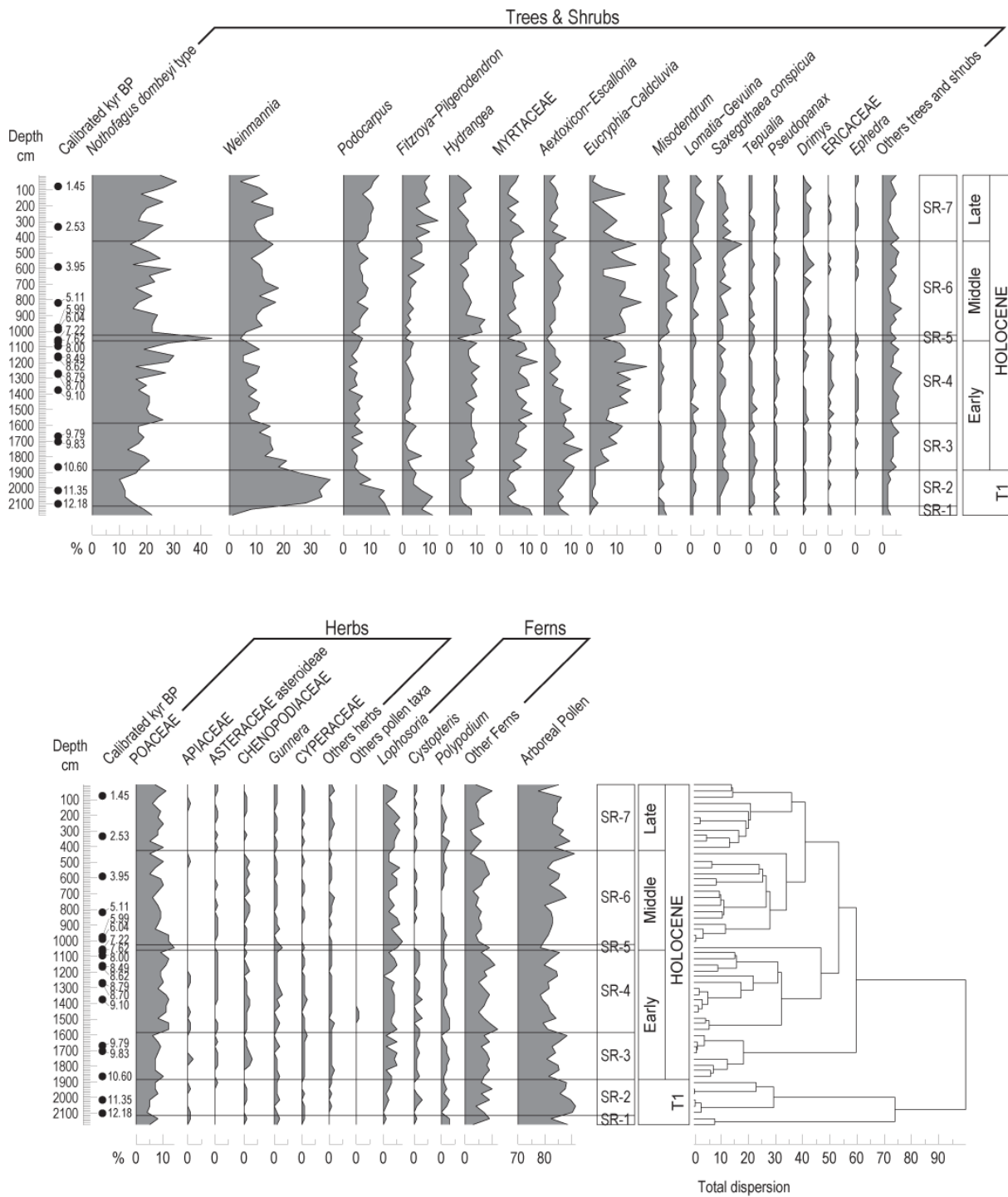


Fig. 3: Pollen percentage diagram from core MD07-3104 according to depth. Calibrated ages on the left and chronostratigraphy with pollen zones are indicated on the right.

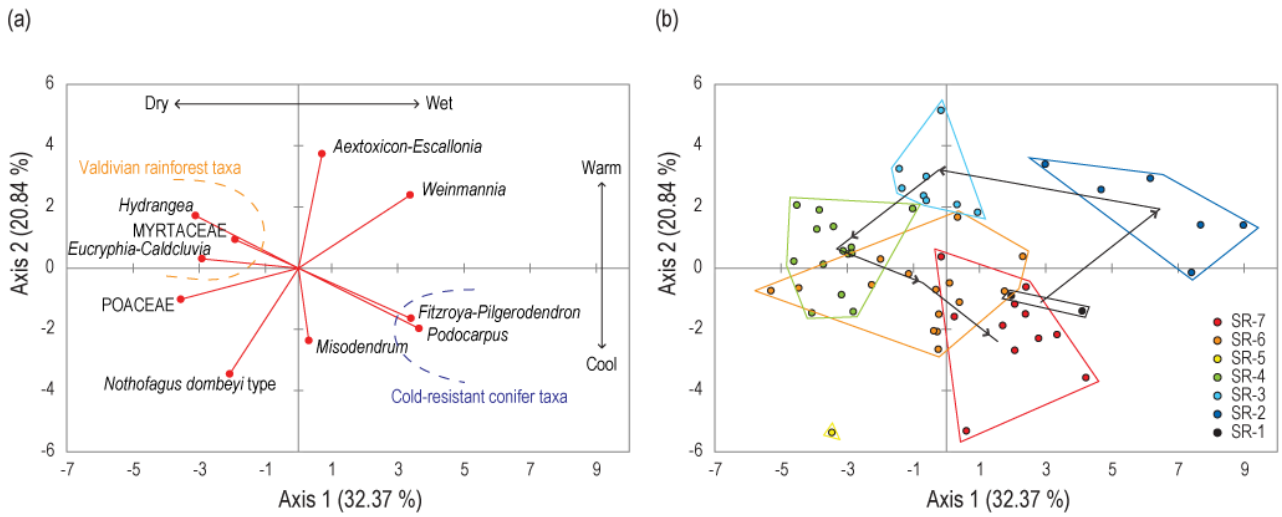


Fig. 5: Principal Component Analysis (PCA). The sum of the axes reaches 53.21% of the original variability (axis 1 = 32.37% and axis 2 = 20.84%). (a) Species biplot shows pollen taxa in pollen analysis with $\geq 5\%$. (b) The polygons correspond to the pollen zones outlined in the pollen diagram, and the arrows correspond to the succession of the pollen zone (the zone SR-5 is disconnected because it does not represent the center of the polygon).

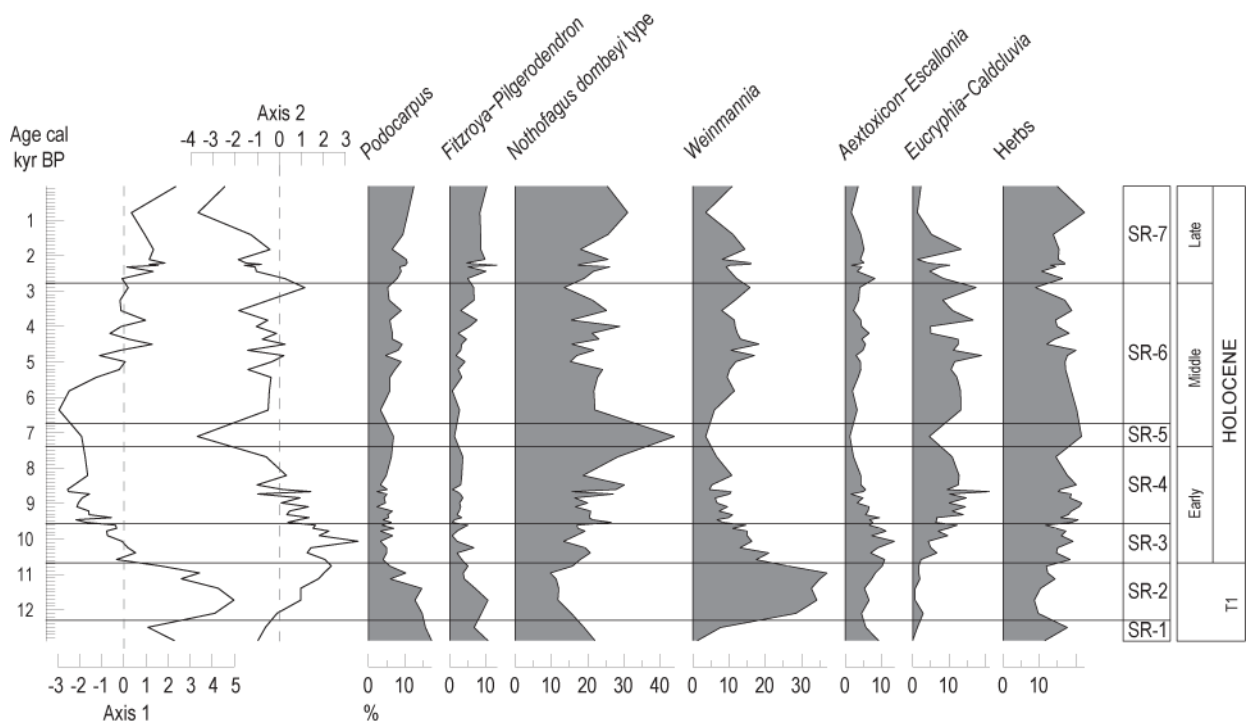


Fig. 6: PCA axis and main pollen taxa percentages curves according to age. On the right are the 7 pollen zones with the chronostratigraphy. Axis 1 shows the opposition between wetter conditions (positive values) and drier conditions (negative values). Axis 2 contrasts warmer conditions (positive values) with cooler conditions (negative values).

Age cal kyr BP	Dominant Taxa	MD073104 Zone	Period	Lago Condorito Zone	Dominant Taxa	Age cal kyr BP
0						0
1	<i>Nothofagus dombeyi</i> type- <i>Podocarpus-Fitzroya/Pilgerodendron-Poaceae</i>	SR-7	H L O C E N E ? L A T E	Co-7b	<i>Weinmannia-Nothofagus dombeyi</i> type- <i>Tepualia</i>	1
2				Co-7a	<i>Nothofagus dombeyi</i> type- <i>Weinmannia-Tepualia</i>	2
3	<i>Nothofagus dombeyi</i> type- <i>Eucryphia-Weinmannia</i>	SR-6	H O L O C E N E ? M I D	Co-6c	<i>Nothofagus dombeyi</i> type- <i>Saxegothaea-Weinmannia-Eucryphia/Caldcluvia</i>	3
4				Co-6b	<i>Nothofagus dombeyi</i> type- <i>Saxegothaea-Weinmannia-Tepualia</i>	4
5				Co-6a	<i>Nothofagus dombeyi</i> type- <i>Saxegothaea-Tepualia-Weinmannia</i>	5
6				Co-5b	<i>Nothofagus dombeyi</i> type- <i>Tepualia-Saxegothaea</i>	6
7	<i>Nothofagus dombeyi</i> type- <i>Poaceae-Podocarpus</i>	SR-5		Co-5a	<i>Tepualia-Nothofagus dombeyi</i> type- <i>Eucryphia/Caldcluvia-Poaceae</i>	7
8	<i>Nothofagus dombeyi</i> type- <i>Eucryphia/Caldcluvia-Poaceae-Myrtaceae</i>	SR-4	H O L O C E N E ? E A R L Y	Co-4b	<i>Tepualia-Eucryphia/Caldcluvia-Nothofagus dombeyi</i> type	8
9				Co-4a	<i>Eucryphia/Caldcluvia-Weinmannia-Poaceae</i>	9
10	<i>Nothofagus dombeyi</i> type- <i>Weinmannia-Aextoxicon/Escallonia-Hydrangea</i>	SR-3		Co-3	<i>Weinmannia-Tepualia-Myrtaceae</i>	10
11	<i>Weinmannia-Nothofagus dombeyi</i> type- <i>Podocarpus</i>	SR-2	T E R M I N A T I O N ? L A S T	Co-2b	<i>Weinmannia-Nothofagus dombeyi</i> type- <i>Hydrangea</i>	11
12				Co-2a	<i>Nothofagus dombeyi</i> type- <i>Myrtaceae-Podocarpus</i>	12
13	<i>Nothofagus dombeyi</i> type- <i>Podocarpus-Myrtaceae-Fitzroya/Pilgerodendron</i>	SR-1		Co-2a	<i>Nothofagus dombeyi</i> type- <i>Myrtaceae-Podocarpus</i>	13

Fig. 7: Comparison between MD07-3104 pollen zone and Lago Condorito pollen zone (Moreno, 2004).

Table Captions

Table 1: Radiocarbon ages obtained by accelerator mass spectrometry (AMS) dating of shell and woody debris in Seno Reloncaví (cores MD07-3104; MD07-3105Cq) and in Reloncaví Fjord (MD07-3107).

Lab. Num.	Sample Name	Core Depth (cm)	Material	14C-Age (BP)	Res. Age (yrs)	Corrected Age (BP)	Age cal. yr. BP (2 σ)
SacA 16367	MD07-3104-I 85	85	wood	1545 \pm 30	0	1545 \pm 30	1452 \pm 48
Poz-20878	MD07-3105 Cq-319	335	shell	2835 \pm 30	400	2435 \pm 30	2526 \pm 130
Poz-20916	MD07-3105 Cq-589	591	wood	3620 \pm 35	0	3620 \pm 35	3950 \pm 72
SacA 16369	MD07-3104-VI 74	824	shell	4865 \pm 30	400	4465 \pm 30	5110 \pm 97
SacA 16370	MD07-3104-VII 75	975	shell	5825 \pm 30	575	5250 \pm 30	5992 \pm 47
SacA 16371	MD07-3104-VII 91	991	shell	5860 \pm 30	575	5285 \pm 30	6041 \pm 51
SacA 16372	MD07-3104-VIII 6	1056	shell	6865 \pm 30	575	6290 \pm 30	7223 \pm 35
SacA 16373	MD07-3104-VIII 16,5	1066,5	shell	7355 \pm 30	575	6780 \pm 30	7624 \pm 32
SacA 16374	MD07-3104-VIII 45	1095	shell	7775 \pm 30	575	7200 \pm 30	8002 \pm 30
SacA 16375	MD07-3104-VIII 110,5	1160,5	shell	8285 \pm 30	575	7710 \pm 30	8486 \pm 53
SacA 16376	MD07-3104-VIII 113,5	1163,5	shell	8415 \pm 30	575	7840 \pm 30	8618 \pm 81
Poz-29330	MD07-3104-IX-1267	1267	shell	8520 \pm 50	575	7945 \pm 50	8788 \pm 130
SacA 16377	MD07-3104-IX 71	1271	shell	8490 \pm 30	575	7915 \pm 30	8700 \pm 55
SacA 16378	MD07-3104-X 25	1375	shell	8745 \pm 30	575	8170 \pm 30	9102 \pm 75
SacA 16379	MD07-3104-XII 21,5	1671,5	shell	9355 \pm 35	575	8780 \pm 35	9790 \pm 145
Poz-29331	MD07-3104-XII-1703	1703	shell	9370 \pm 50	575	8795 \pm 50	9833 \pm 200
SacA 16380	MD07-3104-XIII 65	1865	shell debris	9950 \pm 35	575	9375 \pm 35	10599 \pm 180
Poz-29932	MD07-3104-XIV 2001	2001	wood	10500 \pm 50	0	10500 \pm 50	12394 \pm 250
SacA 16382	MD07-3104-XIV 65,5	2015,5	shell debris	10510 \pm 35	575	9935 \pm 35	11354 \pm 150
SacA 16381	MD07-3104-XIV 151	2101	shell debris	10930 \pm 35	575	10355 \pm 50	12176 \pm 110
Poz-29933	MD07-3107-XVII 2534	2534	wood	4520 \pm 35	0	4520 \pm 35	5182 \pm 90
SacA 16389	MD07-3107-XVII 2534	2534	shell debris	5095 \pm 30	575	4520 \pm 30	5197 \pm 125

Table 2: Pollen zones from core MD07-3104 related to depth, age range, and maximum pollen frequencies associated with climatic changes.

Period	Pollen Zone	Pollen Signature	Climate
Late Holocene	SR-7 5-425 cm 0-2.8 kyr	<i>Nothofagus dombeyi</i> type abundant (15-25%) Increase in <i>Fitzroya-Pilgerodendron</i> (5-10%) and <i>Podocarpus</i> (10%) Slight increase in <i>Lomatia-Gevuina</i> (5%) Decrease in <i>Eucryphia-Caldcluvia</i> (10-15%) and <i>Hydrangea</i> (5-10%)	Cool and humid
	Middle Holocene	SR-6 425-1025 cm 2.8-6.7 kyr	<i>Nothofagus dombeyi</i> type abundant (15-25%) Increase in <i>Weinmannia</i> (10-15%), <i>Eucryphia-Caldcluvia</i> (10-15%), Myrtaceae (5-10%), <i>Hydrangea</i> (10%) Slight increase in <i>Misodendron</i> (5%) and <i>Fitzroya-Pilgerodendron</i> (5%) Oscillations in <i>Podocarpus</i> (5-10%) and <i>Aextoxicon-Escallonia</i> (5%) Slight decrease in Poaceae (10%)
Middle Holocene		SR-5 1025-1060 cm 6.7-7.4 kyr	Peak in <i>Nothofagus dombeyi</i> type (40%) Slight increase in <i>Podocarpus</i> (5-10%) and Poaceae (10-15%) Decrease in other main pollen taxa <i>Weinmannia</i> (5%), <i>Eucryphia-Caldcluvia</i> (5%), Myrtaceae (<5%), <i>Hydrangea</i> (5%) and <i>Aextoxicon-Escallonia</i> (<5%)
	Early Holocene	SR-4 1060-1585 cm 7.4-9.6 kyr	<i>Nothofagus dombeyi</i> type abundant (15-25%) Oscillations in Myrtaceae (10%) and <i>Hydrangea</i> (10%) Increase in <i>Eucryphia-Caldcluvia</i> (10-20%) Decrease in <i>Weinmannia</i> (5-10%) and <i>Aextoxicon-Escallonia</i> (10→5%) Slight increase in Poaceae (10%)
Early Holocene		SR-3 1585-1885 cm 9.6-10.7 kyr	Abrupt decrease in <i>Weinmannia</i> (10-15%) Increase in <i>Nothofagus dombeyi</i> type (20%), <i>Hydrangea</i> (10%) and <i>Aextoxicon-Escallonia</i> (10%) Regular increase in <i>Eucryphia-Caldcluvia</i> and Myrtaceae (5→10%) Low percentages in <i>Podocarpus</i> (5%) and <i>Fitzroya-Pilgerodendron</i> (<5%) Slight increase in <i>Lophosoria</i> (5%)
	Last Termination	SR-2 1885-2115 cm 10.7-12.3 kyr	Abrupt increase in <i>Weinmannia</i> (30%) Decrease <i>Nothofagus dombeyi</i> type (10-15%), Myrtaceae (5%) and <i>Hydrangea</i> (5%) Regular decrease in <i>Fitzroya-Pilgerodendron</i> (10→5%) and <i>Podocarpus</i> (15→5%)
Last Termination		SR-1 2115-2172 cm 12.3-12.9 kyr	High percentages in tree pollen taxa, <i>Nothofagus dombeyi</i> type (20%), <i>Podocarpus</i> (10-15%), <i>Fitzroya-Pilgerodendron</i> (10%), Myrtaceae (10%), <i>Aextoxicon-Escallonia</i> (<10%), <i>Weinmannia</i> (<10%), <i>Hydrangea</i> (<10%) and <i>Eucryphia-Caldcluvia</i> (<5%) Low percentages in herbs pollen taxa (<5%), Poaceae (5-10%) <i>Lophosoria</i> (<5%)